INSTITUTE OF PHYSICS PUBLISHING NANOTECHNOLOGY
Nanotechnology **18** (2007) 015404 (4pp) doi:10.1088/0957-4484/18/1/015404

Drastic ion-implantation-induced intermixing during the annealing of self-assembled InAs/InP(001) quantum dots

C Dion[1,2], P Desjardins[1], M Chicoine[3], F Schiettekatte[3], P J Poole[2] and S Raymond[2]

[1] Regroupement Québécois sur les Matériaux de Pointe (RQMP), Département de génie physique, École Polytechnique de Montréal, Montréal, QC, H3C 3A7, Canada
[2] Institute for Microstructural Sciences, National Research Council, Ottawa, ON, K1A 0R6, Canada
[3] Regroupement Québécois sur les Matériaux de Pointe (RQMP), Département de Physique, Université de Montréal, Montréal, QC, H3C 3J7, Canada

E-mail: carolyne.dion@polymtl.ca

Received 8 September 2006, in final form 2 November 2006
Published 8 December 2006
Online at stacks.iop.org/Nano/18/015404

Abstract
This work examines the influence of post-growth phosphorus implantation followed by rapid thermal annealing on the photoluminescence (PL) emission from self-assembled InAs/InP(001) quantum dots (QDs). Upon annealing, the spectra reveal an atypical evolution, showing an increase in the emission bandwidth and the rise of a InAsP quantum-well-like peak. The overall emission exhibit a blueshift whose magnitude increases with annealing temperature and fluence up to ∼325 meV. The temperature threshold for a detectable PL shift, 400 °C, is considerably lower than the 725 °C value for unimplanted samples, thereby demonstrating the potential of ion-implantation-induced intermixing for spatially selective band gap tuning of InAs/InP QDs.

1. Introduction

Because of their promising high characteristic temperature and low threshold current density, lasers based on InAs/InP(001) quantum dots (QDs) are attractive building blocks for the next generation of optical networks operating in the 1.5 μm range [1]. As the development of these technologies requires the integration of lasers with various emission wavelengths on a single chip, spatially selective band gap tuning of QD structures is becoming a critical issue. Band gap tuning can be achieved after epitaxial growth through atomic interdiffusion, or intermixing, at the QD/barrier interface. This modifies the confinement profile and alters the QD energy levels, thereby inducing a shift of the emission spectra. The simplest way to implement band gap tuning consists of subjecting the sample to rapid thermal annealing (RTA). However, thermal intermixing does not provide the ability to address a specific region of the sample for monolithic integration. To this end spatially selective intermixing (SSI), involving either localized heating or sectional creation/suppression of point defects in the structure to enhance/inhibit intermixing, is required. Examples of SSI techniques include laser irradiation [2, 3], dielectric capping (often referred to as impurity–free vacancy disordering) [2, 4], grown-in defects (GID) [5, 6] and ion implantation. This latter technique has successfully been used for the band gap modification of quantum wells (QWs) in various semiconductor systems (see for examples [7, 8]). Its use in lower-dimensionality systems has so far been limited to In(Ga)As/(Al)GaAs QDs [9–12] and InAs/InP quantum sticks [13]. For InAs/InP QDs, recent work by Barik *et al* [14] has shown that proton implantation is promising for tuning the QD emission properties. However, intermixing studies in InAs/InP QDs are still in their infancy and more work is clearly required for better control and understanding of the ion-implantation-induced intermixing dynamics.

In this paper we examine the influence of low-energy phosphorus implantation followed by RTA on the photoluminescence (PL) spectra of InAs/InP(001) QDs grown by metalorganic vapour phase epitaxy (MOVPE) and

chemical beam epitaxy (CBE). After ion-implantation-induced intermixing, drastic modifications of the PL spectra are observed in samples grown using both techniques. Important PL shifts and bandwidth broadening are achieved in implanted samples subjected to RTA, a very promising result for SSI in InAs/InP QD-based structures.

2. Experimental section

Self-assembled InAs QDs were grown using MOVPE and CBE. MOVPE samples were grown on Fe-doped InP(001) misoriented by 2° towards [110]. Pd-purified H_2 was used as the carrier gas with trimethylindium (TMIn), tertiarybutylphosphine (TBP) and tertiarybutylarsine (TBAs) as precursors. Following the deposition of a 200 nm thick InP buffer layer at 600 °C, the temperature was lowered to 500 °C under a TBP/H_2 ambient. Then, 3.5 monolayers (ML) of InAs were deposited followed by a 60 s growth interruption under a TBAs/H_2 ambient to allow QD formation. A 5 nm thick InP layer was then deposited in order to freeze the evolution of the InAs layer morphology. Finally, the temperature was increased to 600 °C and a 200 nm thick InP capping layer was deposited. CBE samples were grown on Fe-doped InP(001) using TMIn, arsine and phosphine without a carrier gas. These samples consisted of a 190 nm thick InP buffer layer, 2.2 ML of InAs followed by a 60 s growth interruption and a 150 nm thick InP cap layer, all grown at 495 °C.

The as-grown samples were cleaved into pieces of approximately 5 × 5 mm^2. Except for one piece used as a reference sample, each piece was implanted using 30 keV P^- ions to avoid introducing foreign atoms into the structure, with fluences Φ ranging from 10^{11} to 10^{14} cm^{-2}. The ion energy was chosen based on SRIM 2000 simulations [15] in order to locate the implantation damage in the top 120 nm of the InP capping layer. Implantations were performed at 7° off the ⟨001⟩ direction to minimize channelling effects, and at a substrate temperature of 200 °C to avoid surface amorphization [16]. Each piece was then subjected to a series of 60 s anneals, where the annealing temperature (T_a) was progressively increased from 400 to 600 °C by 50 °C intervals. RTAs were performed on InP proximity capped samples using an A.G. Associates Heatpulse 410 system in a VLSI grade nitrogen atmosphere.

The interdiffusion process was analysed by PL spectroscopy realized at 77 K. Measurements on the MOVPE samples were carried out using the 632.8 nm line of a HeNe laser and acquired with a Fourier transform infrared spectrometer with a thermoelectrically cooled InGaAs detector. For the CBE samples, the 532 nm emission of a Nd:YVO_4 laser was used as the excitation source while a double grating spectrometer with a LN_2-cooled Ge detector was used for signal collection. The resolution of these systems was comparable, 4 and 3 meV respectively. In both cases, the probe spot was about 50 μm in diameter, resulting in excitation power densities of 20 and 50 W cm^{-2} for MOVPE and CBE samples, respectively. These power densities were sufficiently low to prevent any distortion of the spectra by excess carrier population in the QDs.

3. Results and discussion

Figure 1 presents PL spectra from CBE and MOVPE QDs as a function of T_a for both unimplanted and implanted

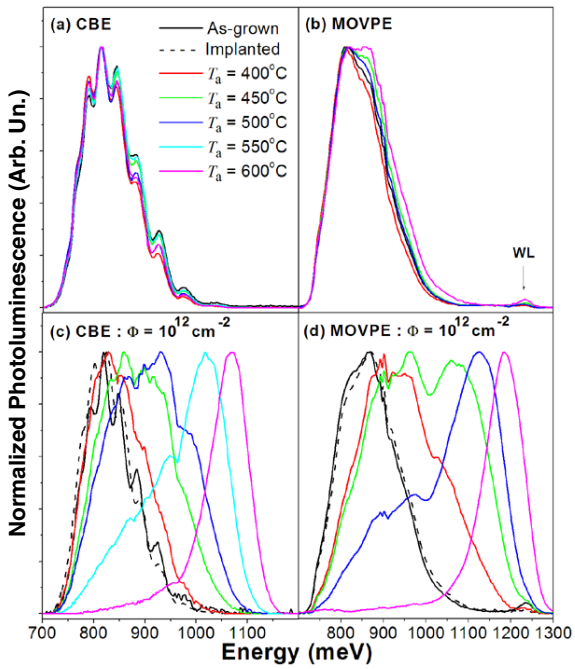

Figure 1. PL spectra from as-grown and annealed samples as a function of annealing temperature T_a from 400 to 600 °C: (a) CBE, unimplanted; (b) MOVPE, unimplanted; (c) CBE, $\Phi = 10^{12}$ cm^{-2}; (d) MOVPE, $\Phi = 10^{12}$ cm^{-2}.

(This figure is in colour only in the electronic version)

samples. Figures 1(a) and (b) demonstrate that for both growth techniques, the as-grown samples are characterized by a broad emission peak centred at around 850 meV arising from the electron–heavy-hole transition of an ensemble of QDs. The CBE PL spectra shown in figure 1(a) are the superposition of up to nine inhomogeneously broadened peaks which are attributed to QD families having the same thickness in terms of an integer number of MLs [17, 18]. Variations in interface roughness, strain field, lateral size and composition contribute to the inhomogeneous broadening of the emission line of a given family. For the MOVPE samples, figure 1(b) shows that individual island families cannot be resolved due to a higher inhomogeneous broadening. The low-intensity peak observed at 1230 meV in the MOVPE sample is attributed to the wetting layer (WL) emission [19]. This peak is not observed in the CBE sample, which is consistent with a higher QD density and/or a better carrier transfer from WL to QD [20]. Figures 1(a) and (b) further show that successive 60 s anneals in the 400 to 600 °C temperature range performed on unimplanted samples result in negligible changes in the PL emission, in agreement with previous studies that revealed a T_a threshold of about 725 °C for a significant PL shift in InAs/InP-based quantum structures [2, 17, 21].

Figures 1(c) and (d) reveal that for $\Phi = 10^{12}$ cm^{-2} no significant changes in the shape and wavelength peak from the PL spectra of the as-implanted samples can be observed, thereby suggesting that no intermixing occurred during that processing step. However, upon annealing significant changes arise in the PL spectra. For both types of sample the global maximum of the QD emission spectra shifts monotonically with T_a while the overall emission bandwidth progressively

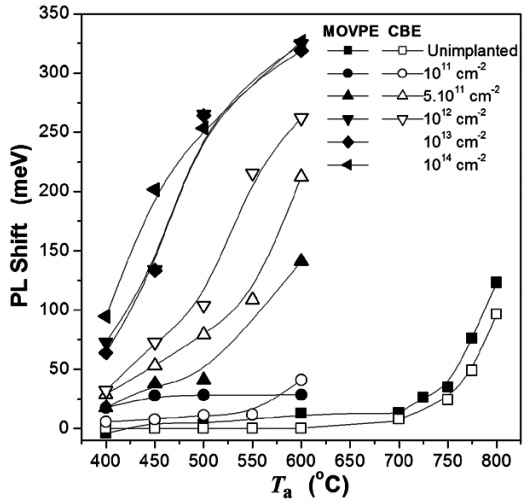

Figure 2. PL shift as a function of T_a for unimplanted and implanted samples (fluence ranging from 10^{11} to 10^{14} cm^{-2}).

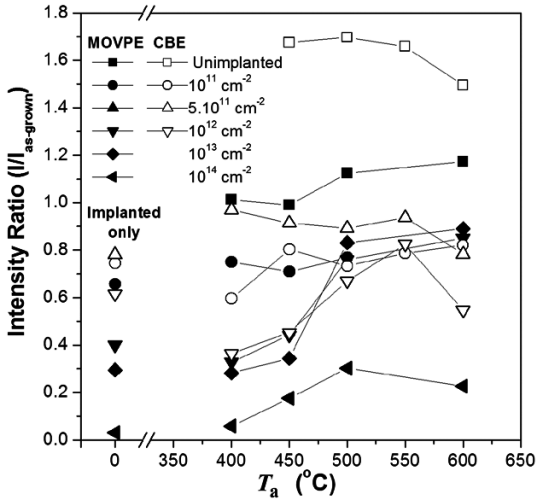

Figure 3. PL peak intensity normalized to that of the as-grown sample as a function of T_a for reference samples as well as QD structures implanted with fluences between 10^{11} and 10^{14} cm^{-2}.

increases. For example, the full-width at half-maximum of the PL spectra displayed in figure 1(d) increases by 70 and 140 meV after RTA treatments at 400 and 450 °C, respectively. For the CBE sample, one further notes that QD family peaks can no longer be resolved [17]. Next, PL spectra reveal the gradual emergence of a high-energy peak centred at 1020 and 1130 meV, respectively, for CBE and MOVPE samples annealed at 550 and 500 °C. Finally, after annealing at 600 °C, the spectra progressively transform into a much narrower peak with an energy approaching that of the WL (∼1100 meV for the CBE-grown sample [22]).

Figure 2 shows the influence of T_a and ion fluence on the PL shift determined by comparing the global maximum peak position of PL spectra in as-grown and treated samples. The PL emission from unimplanted samples is seen to remain stable up to approximately 725 °C [17]. In contrast, ion implantation reduces by ∼300 °C the T_a required to induce a PL shift. This reduction is much more pronounced than that reported in the widely studied InGaAs/InP QW structures where ion implantation led to a decrease in threshold temperatures for intermixing by only 50 °C [23]. The maximum shifts obtained following the 600 °C anneal are 250 and 325 meV for the CBE and MOVPE samples, respectively. The larger PL shifts achieved in the MOVPE samples are probably due to an *in situ* annealing resulting from the higher temperature used during growth of the InP capping layer. Such *in situ* annealing was recently shown to reduce QD thermal stability, and give hence higher PL shifts [24]. Figure 2 further indicates that PL shifts increase sharply with fluences between 10^{11} and 10^{12} cm^{-2} and tend to saturate thereafter. One should note that these fluences are two orders of magnitude smaller than those required for implantation-induced intermixing in InP-based QW structures [23].

The evolution of the PL peak intensity ratio as a function of T_a and fluence is shown in figure 3. First, this figure reveals that unimplanted CBE samples exhibit a higher increase in PL signal intensity upon annealing than MOVPE structures. Recalling that point defects act as non-radiative recombination centres and that their annihilation under annealing produces an increase in PL intensity, our results provide evidence that CBE layers contained a more important concentration of as-grown defects. This is a reasonable conclusion since MOVPE samples were grown at a higher temperature. Figure 3 further shows that PL intensity immediately after P^- implantation is significantly reduced for both types of sample, therefore confirming the formation of implantation defects in the capping layer. For implanted samples, the evolution of the PL intensity upon annealing is thus a combined effect of grown-in defects annihilation and implantation damage recovery. In the case of MOVPE samples, the signal progressively increases upon annealing to about 80% of the as-grown intensity for fluences of 10^{13} cm^{-2} and below. By sharp contrast, for a fluence of 10^{14} cm^{-2}, only 20% of the signal is recovered, probably because of important implantation damage accumulation in the InP capping layer. For CBE samples implanted with fluences below 10^{12} cm^{-2}, the PL intensity reaches about 80% of that of as-grown samples. Because of the noticeable contribution of grown-in defect annihilation on the evolution of the PL intensity for such samples, one can deduce from figure 3 that less than 50% of the implantation damage was recovered upon annealing. This is lower than in the MOVPE samples, which may suggest that grown-in defects impede implantation damage recovery.

Our results clearly demonstrate that implantation of heavy ions in InP is a promising technique for emission tuning of self-assembled InAs/InP(001) QDs. More specifically, important PL shifts can be obtained in implanted samples at T_a well below the onset for intermixing in unimplanted samples. This is attributed to the presence of highly mobile implantation-induced defects that provoke a substantial surge of group V intermixing during annealing [7, 23]. Generally, these defects are known to degrade device performance and reliability. However, the results displayed in figure 3 show that the use of low implantation fluences allows a respectable recovery of the optical efficiency after annealing. We also point out that despite the fact that CBE and MOVPE samples were grown under different conditions, have different InAs coverages (2.2 and 3.5 ML) and that the implantation damage is located at slightly different distances from the QD layer due

to different cap thickness (150 and 200 nm), our results show that both structures behave similarly upon ion-implantation-induced intermixing.

One must, however, be careful in the physical interpretation of the PL spectra after such treatment. In fact, the peculiar evolution of the PL characteristics shown in figure 1 indicates a significant bandwidth broadening resulting from an augmentation in inhomogeneity of the QDs. Furthermore, as the amount of intermixing is increased, a progressive rise of a high-energy shoulder that slowly transforms into a much narrower peak similar to QW emission is observed. This suggests that islands tend to dissolve within the WL to form a non-uniform InAsP QW. This is in sharp contrast with other results achieved using other intermixing techniques [6, 17]. Indeed, for GID and RTA treatments, the PL evolution is interpreted in terms of QD families shifting at similar rates for given annealing conditions as they retain their structural integrity.

4. Conclusion

In summary, we have found that damage produced by phosphorus implantation in the capping layer dramatically increases interdiffusion in InAs/InP(001) QDs, as evidenced by both the temperature threshold for PL shift of 400 °C and the large PL shifts of 325 meV obtained after annealing at 600 °C. Since no significant PL shifts could be obtained below 725 °C in the case of unimplanted samples, this clearly demonstrates the potential of ion-implantation-induced intermixing for spatially selective band gap tuning in monolithic integration. Implanted samples further exhibit a unique evolution of their PL spectra under annealing through the appearance of an InAsP QW-like peak and significant bandwidth broadening, a key finding towards our understanding of the interdiffusion dynamics in InAs/InP QDs.

Acknowledgments

The authors acknowledge financial support from the Canada Research Chair program, the Natural Science and Engineering Research Council of Canada and the Fonds Québécois de Recherche sur la Nature et les Technologies, and NanoQuébec.

References

[1] Delorme F 1998 *IEEE J. Quantum Electron.* **34** 1706
[2] Chia C K, Chua S J, Tripathy S and Dong J R 2005 *Appl. Phys. Lett.* **86** 51905
[3] Djie H S, Ooi B S and Gunawan O 2006 *Appl. Phys. Lett.* **89** 81901
[4] Fu L, Lever P, Tan H H, Jagadish C, Reece P and Gal M 2003 *Appl. Phys. Lett.* **82** 2613
[5] Jiang W H, Thompson D A, Hul'ko O, Robinson B J and Mascher P 2006 *J. Vacuum Sci. Technol.* A **24** 700
[6] Dion C, Desjardins P, Schiettekatte F, Poole P J and Raymond S 2006 *Appl. Phys. Lett.* **89** 131905
[7] Charbonneau S *et al* 1998 *IEEE J. Sel. Top. Quantum Electron.* **4** 772
[8] Goldberg R D *et al* 1997 *Nucl. Instrum. Methods Phys. Res.* B **127/128** 418
[9] Lever P, Tan H H, Jagadish C, Reece P and Gal M 2003 *Appl. Phys. Lett.* **82** 2053
[10] Surkova T *et al* 2001 *J. Appl. Phys.* **89** 6044
[11] Ji Y, Wei Lu, Chen G, Chen X and Wang Q 2003 *J. Appl. Phys.* **93** 1208
[12] Djie H S, Ooi B S and Aimez V 2006 *J. Cryst. Growth* **288** 40
[13] Salem B, Aimez V, Morris D, Turala A, Regreny P and Gendry M 2005 *Appl. Phys. Lett.* **87** 241115
[14] Barik S, Tan H H and Jagadish C 2006 *Appl. Phys. Lett.* **88** 223101
[15] Ziegler J F, Biersack J P and Littmark U 1985 *The Stopping and Ion Range of Ions in Matter* (New York: Pergamon)
[16] Carmody C, Tan H H and Jagadish C 2003 *J. Appl. Phys.* **93** 4468
[17] Girard J F, Dion C, Desjardins P, Allen C N, Poole P J and Raymond S 2004 *Appl. Phys. Lett.* **84** 3382
[18] Sakuma Y, Takemoto K, Hirose S, Usuki T and Yokoyama N 2005 *Physica* E **26** 81
[19] Leonelli R *et al* 1993 *Phys. Rev.* B **48** 11135
[20] Leon R and Fafard S 1998 *Phys. Rev.* B **58** 1726
[21] Sallese J M *et al* 1994 *Appl. Phys. Lett.* **65** 341
[22] Poole P J, McCaffrey J, Williams R L, Lefebvre J and Chithrani D 2001 *J. Vac. Sci. Technol.* B **19** 1467
[23] Aimez V, Beauvais J, Beerens J, Morris D, Lim H S and Ooi B-S 2002 *IEEE J. Sel. Top. Quantum Electron.* **8** 870
[24] Djie H S *et al* 2006 *J. Appl. Phys.* **100** 33527